Transcriptional Profiling Shows Altered Expression of Wnt Pathway– and Lipid Metabolism–Related Genes as Well as Melanogenesis-Related Genes in Melasma

Hee Young Kang[1,5], Itaru Suzuki[2,5], Dong Jun Lee[1], Jaehyun Ha[3], Pascale Reiniche[2], Jérôme Aubert[2], Sophie Deret[2], Didier Zugaj[2], Johannes J. Voegel[2] and Jean-Paul Ortonne[4]

Melasma is a commonly acquired hyperpigmentary disorder of the face, but its pathogenesis is poorly understood and its treatment remains challenging. We conducted a comparative histological study on lesional and perilesional normal skin to clarify the histological nature of melasma. Significantly, higher amounts of melanin and of melanogenesis-associated proteins were observed in the epidermis of lesional skin, and the mRNA level of tyrosinase-related protein 1 was higher in lesional skin, indicating regulation at the mRNA level. However, melanocyte numbers were comparable between lesional and perilesional skin. A transcriptomic study was undertaken to identify genes involved in the pathology of melasma. A total of 279 genes were found to be differentially expressed in lesional and perilesional skin. As was expected, the mRNA levels of a number of known melanogenesis-associated genes, such as tyrosinase, were found to be elevated in lesional skin. Bioinformatics analysis revealed that the most lipid metabolism-associated genes were downregulated in lesional skin, and this finding was supported by an impaired barrier function in melasma. Interestingly, a subset of Wnt signaling modulators, including Wnt inhibitory factor 1, secreted frizzled-related protein 2, and Wnt5a, were also found to be upregulated in lesional skin. Immunohistochemistry confirmed the higher expression of these factors in melasma lesions.

Journal of Investigative Dermatology (2011) **131,** 1692–1700; doi:10.1038/jid.2011.109; published online 12 May 2011

INTRODUCTION

Melasma is a common acquired hyperpigmentary disorder characterized by light- to dark-brown patches on the face primarily caused by increased melanin deposition in the epidermis (Kang *et al.*, 2002; Grimes *et al.*, 2005). Melanocytes within affected skin are larger, more dendritic, and contain more melanosomes than melanocytes of unaffected skin, which suggests that melanocytes are active in melasma. These findings correlate well with the findings of an *in vivo* reflectance confocal microscopic studies of melasma, which have shown a significantly higher level of epidermal pigmentation in lesional skin as compared with perilesional normal skin (Kang *et al.*, 2010).

The pathogenesis of melasma remains largely unknown and its treatment challenging. A recent large-scale survey of 324 melasma-affected women suggested that a combination of known triggers, such as, pregnancy, hormonal birth control, a family history, and sun-exposure affect the onset of melasma (Ortonne *et al.*, 2009). Several histopathological studies suggested that several protein factors and cellular compartments have pathogenic roles. Im *et al.* (2002) found that α-melanocyte-stimulating hormone (α-MSH) protein levels are higher in melasma lesions, and Kang *et al.* (2006) reported that stem cell factor expression from fibroblasts and fibroblast numbers were higher in lesional skin. Furthermore, Kim *et al.* (2007) showed that lesions tend to contain more blood vessels, and suggested that vascular endothelial growth factor promotes the prominent vascularization of melasma lesions.

However, although several histological studies have been performed on different protein markers, the pathogenesis of melasma is far from being revealed. In the present study, we performed large-scale gene expression profiling to

[1]*Department of Dermatology, Ajou University School of Medicine, Suwon, Korea;* [2]*Scientific Division, Galderma R&D, Sophia-Antipolis, France;* [3]*Scientific Division, I.E.C. Korea, Suwon, Korea and* [4]*Department of Dermatology, Archet-2 Hospital, University of Nice, Nice, France*

[5]*These authors contributed equally to this work.*

Correspondence: Jean-Paul Ortonne, Department of Dermatology, Archet-2 Hospital, 151 Route St Antoine de Ginestiere, BP 3079, 06202 Nice, France. E-mail: ortonne@unice.fr

Abbreviations: DCT, dopachrome tautomerase; IHC, immunohistochemistry; ISH, in situ *hybridization; MITF, microphthalmia-associated transcription factor; SFRP, secreted frizzled-related protein; SILV, silver; TEWL, transepidermal water loss; TYR, tyrosinase; TYRP1, tyrosinase-related protein 1; WIF1, WNT inhibitory factor 1*

Received 9 November 2010; revised 30 January 2011; accepted 11 February 2011; published online 12 May 2011

investigate the pathogenesis of melasma. In the first part of this study, histological analysis was performed to clarify the nature of melasma and to justify a subsequent transcriptomic study.

RESULTS

Histochemical and immunohistochemical evaluations and *in situ* hybridization of *TYRP1*

Hematoxylin–eosin and Fontana–Masson staining were performed to evaluate the general morphology of and the quantity/distribution of melanin in the skin samples (Figure 1a). Hematoxylin–eosin staining showed no significant differences in general morphology between lesional and perilesional skin. Fontana–Masson staining demonstrated that epidermal melanin was markedly increased in lesional skin. The melanin was concentrated in the basal layer, but was also distributed throughout the epidermis. Dermal melanin levels were too low to be of clinical significance. Immunohistochemical staining was performed for tyrosinase (TYR), tyrosinase-related protein 1 (TYRP1), dopachrome tautomerase (DCT), silver (SILV), microphthalmia-associated transcription factor (MITF), and SOX10 (Figure 1b). The levels of TYR, TYRP1, DCT, and SILV, which are used as markers of melanogenic activity, were higher in lesional skin (Figure 1c). On the other hand, numbers of melanocytes, as determined by the expressions of MITF and SOX10, were not significantly different in lesional and perilesional skin (Figure 1c). TYRP1 *in situ* hybridization (ISH) was performed to determine whether its elevated protein level in lesional skin was due to an increase in its mRNA level (Figure 1d). In three patients, the mRNA level of *TYRP1* was elevated in lesional skin, but in the other four, no significant difference was observed. Nevertheless, these findings indicated that the increased protein levels observed by immunohistochemistry (IHC) were at least partly due to transcriptional increases, which reinforces the importance of performing transcriptomic analysis and the use of TYRP1 as a positive control.

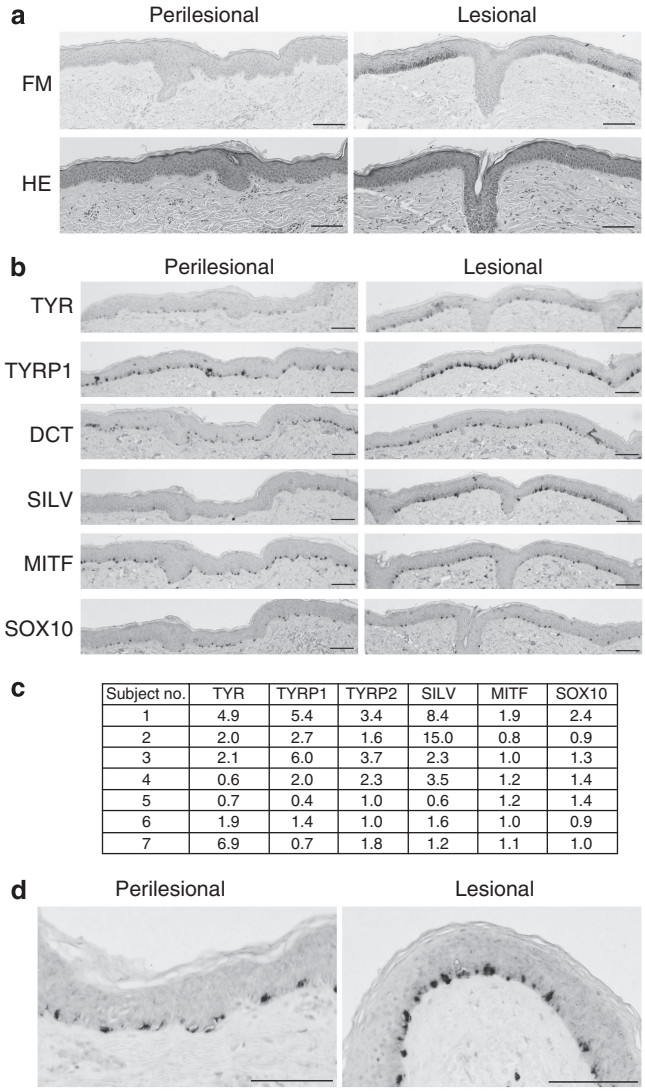

c

Subject no.	TYR	TYRP1	TYRP2	SILV	MITF	SOX10
1	4.9	5.4	3.4	8.4	1.9	2.4
2	2.0	2.7	1.6	15.0	0.8	0.9
3	2.1	6.0	3.7	2.3	1.0	1.3
4	0.6	2.0	2.3	3.5	1.2	1.4
5	0.7	0.4	1.0	0.6	1.2	1.4
6	1.9	1.4	1.0	1.6	1.0	0.9
7	6.9	0.7	1.8	1.2	1.1	1.0

Figure 1. Histochemical/immunohistochemical evaluations and messenger RNA levels of tyrosinase-related protein 1 (TYRP1). (**a**) Hematoxylin–eosin (HE) staining showed no major difference in the general morphology or cytology of skin samples. Fontana–Masson (FM) staining showed an obvious increase in epidermal melanin in lesional skin. In these subjects, we did not observe significant amounts of dermal melanin (bar = 100 μm). (**b**) Melanogenesis-associated factors (tyrosinase (TYR), TYRP1, dopachrome tautomerase (DCT), and silver (SILV)) and melanocyte-specific transcription factors (microphthalmia-associated transcription factor (MITF) and SOX10) were evaluated by immunohistochemistry. TYR is stained red and the other proteins are stained blue (see color figure online). The melanogenesis-associated factors were found to be upregulated in lesional skin (bar = 100 μm). (**c**) Numbers represent fold increases in lesional skin as compared with perilesional skin of same patients as determined by image analysis. Image analysis results corresponded well with visual assessments. Interestingly, numbers of melanocytes determined by MITF and SOX10 immunostaining were not significantly different. (**d**) Signals were observed in cells in the basal layer epidermis corresponding to the distribution of melanocytes. The mRNA levels of TYRP1 were elevated in lesional skin (bar = 100 μm).

Identification of genes differentially expressed in lesional skin

Biostatistical analysis of 10 paired samples showed that 131 probe sets were differentially expressed in lesional and perilesional skin. Furthermore, hierarchical clustering analysis of these 131 probe sets separated lesional and perilesional samples, and revealed the existence of two subgroups of samples (Figure 2). The gene expression of one subgroup of six patients was more affected than those of the other four patients. In addition, this transcriptomic classification was found to be well correlated with clinical data (delta *L* values: data not shown). A second statistical analysis of the six paired samples identified 339 probe sets (279 genes) to be differentially expressed in lesional and perilesional skin (fold modulation of >1.4 or <0.71, $P<0.05$); 187 probe sets were upregulated and 152 probe sets downregulated in lesional skins. The 20 most up- and downregulated probe sets are listed in Table 1, and as was expected based on our IHC and ISH results, the melanogenesis-associated genes (*SILV*, *TYRP1*, *melan-A* (*MLANA*), *TYR*) were included in our upregulated genes list. The upregulated genes included *WNT inhibitory factor 1* (*WIF1*), which is an antagonist of Wnt signaling (Kawano *et al.*, 2003) and *leucine-rich repeat-containing G protein-coupled receptor 5*,

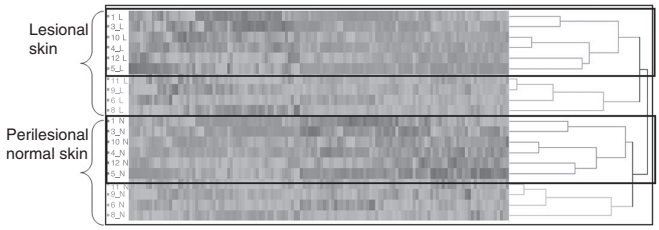

Figure 2. Hierarchical clustering. Hierarchical clustering analysis was performed on 131 probe sets found to be differentially expressed in lesional and perilesional skin. The results obtained revealed the existence of two subgroups, in which one subgroup of six patients (box) was more affected in terms of gene expressional changes than the other subgroup (four patients). Red and blue (see color figure online) represent up- and downregulated genes, respectively.

which is involved in Wnt signaling as a Wnt target gene (Garcia *et al.*, 2009). Genes known to be involved in fibroblast and keratinocyte proliferation, namely, *cartilage oligomeric matrix protein* (*COMP*), *insulin-like growth factor-binding protein 3* (*IGFBP3*), and *serpin peptidase inhibitor, clade B* (*ovalbumin*) *member 3* (also known as *SCCA1*; Enk *et al.*, 2004; Edmondson *et al.*, 2005; Hesselstrand *et al.*, 2008) were also among the top 20 upregulated genes.

Bioinformatics analysis: gene ontology and biological pathways

We performed gene ontology analysis using the web-based application GOTM (http://bioinfo.vanderbilt.edu/gotm/) on the 279 differentially expressed genes. Melanin biosynthesis, lipid metabolism, and prostaglandin metabolism were identified as the most affected biological processes (Table 2). All four genes involved in melanin biosynthesis (*TYR*, *TYRP1*, *DCT*, and *SILV*) were upregulated. Whereas, most of the lipid metabolism associated genes, such as *PPARA*, *arachidonate 15-lipoxygenase, type B*, *diacylglycerol O-acyltransferase2-like 3*, and *PPAR gamma coactivator 1 alpha*, were downregulated. Notably, *prostaglandin-endoperoxide synthase 1*, a key participant in prostaglandin synthesis, was upregulated.

A literature-based molecular network analysis on the 279 differentially expressed genes identified the MITF-associated pathway as the most significantly modified pathway. All of the following clustered members of this pathway were upregulated: *MITF*, transient receptor potential cation channel, subfamily M, member 1, paired box 6, empty spiracles homeobox 2, *SILV*, *TYRP1*, *MLANA*, and *TYR* (Supplementary Figure S1 online). A matrix metallopeptidase (MMP2)-related pathway, including *MMP2*, *endothelin-3*, and *endothelin receptor B* (1.46-, 1.41-, and 1.38-fold inductions, respectively), was also identified. Furthermore, a subset of Wnt pathway modulator genes, i.e., *WIF1*, *secreted frizzled-related protein 2* (*SFRP2*), and *WNT5a*, were found to be significantly upregulated in lesional skin (2.87-, 1.76-, and 1.44-fold inductions, respectively). Although their fold changes did not reach our cutoff thresholds, the mRNA levels of *Dickkopf* (*DKK*)*1*, *DKK2*, and *DKK3* were also slightly increased (by 1.22-, 1.35-, and 1.23-fold, respectively).

Barrier recovery was delayed in lesional skin

To further investigate the involvements of lipid metabolism-related genes in melasma, we measured the barrier functions of lesional and perilesional skins by measuring transepidermal water losses (TEWLs; Figure 3). Basal TEWL (T_{base}) values of lesional skins did not differ significantly from those of perilesional skins (13.5 ± 4.0 vs. 15.6 ± 4.6, $P = 0.210$). However, TEWL values after barrier perturbation were significantly higher for lesional skins (79.5 ± 40.9% vs. 143.2 ± 116.4%, $P = 0.014$). A significantly delayed barrier recovery rate was demonstrated by lesional skins (76.3 ± 12.3% vs. 62.5 ± 22.8%, $P = 0.043$).

Immunohistochemistry for Wnt signaling-associated factors

We performed IHC for the Wnt signaling-associated factors (WIF1, SFRP2, and WNT5a) to determine their distributions and expression levels in normal skin (Figure 4). WIF1 was found to be faintly expressed in the basal layer of the epidermis, whereas SFRP2 was distributed in all layers of the epidermis in a mosaic pattern. Wnt5a was also expressed in the epidermis. Interestingly, melanocytes were positive for WIF1 and Wnt5a, and dermal fibroblasts and endothelial cells were positive for all three proteins. In the five of eight patients, the protein levels of WIF1 were stronger in the melanocytes of lesional skin samples than in those of perilesional skin samples (Figure 4a and b). Furthermore, SFRP2 immunoreactivity around dermal fibroblasts seemed to be higher in the lesional skin (Figure 4c and d), and Wnt5a immunoreactivity was also higher in the basal layer and around fibroblasts in lesional skin (Figure 4e and f). Taken together, the expressions of WIF1, SFRP2, and WNT5a protein were upregulated in lesional skin.

DISCUSSION

This study demonstrates that increased epidermal pigmentation is the main physiopathological observation in melasma affected. The protein levels of melanogenesis-associated factors (TYR, TYRP1, DCT, and SILV) were increased in melasma lesions, indicating higher melanogenic activity in lesional skin. The amount of dermal melanin observed was too low to be of clinical significance, which concurs with previous reports that epidermal hyperpigmentation is the hallmark of melasma (Kang *et al.*, 2002, 2010; Grimes *et al.*, 2005). Also, it should be considered that dermal melanin is commonly found in normal facial skin as well as melasma in skin types III to V. Considering our patients were Caucasian, it is not surprising they had little dermal melanin.

The numbers of melanocytes were not significantly increased in melasma. As melanocytes are dendritic cells, the use of cytoplasmic proteins, such as TYR and TYRP1, as markers for counting melanocytes can be misleading. In the present study, we used two nuclear markers of melanocytes (MITF and SOX10) to count melanocytes to avoid this problem. The results obtained with these markers were consistent, which indicates that numbers of melanocytes are no different in melasma lesions. These results show that the increased epidermal melanin observed in melasma lesions is due to increased melanogenesis in individual melanocytes

Table 1. The 20 most up- and downregulated genes ranked according to mean value

Probe set	Gene symbol	Gene title	UNIGENE	Fold induction (geometric mean)
(A) Upregulated				
224209_s_at	*GDA*	*Guanine deaminase*	Hs.494163	3.087
209848_s_at	*SILV*	*Silver homolog (mouse)*	Hs.95972	3.040
205694_at	*TYRP1*	*Tyrosinase-related protein 1*	Hs.270279	2.881
204712_at	*WIF1*	*WNT inhibitory factor 1*	Hs.284122	2.871
1553081_at	*WFDC12*	*WAP four-disulfide core domain 12*	Hs.352180	2.853
235795_at	*PAX6*	*Paired box 6*	Hs.591993	2.747
205229_s_at	*COCH*	*Coagulation factor C homolog, cochlin (Limulus polyphemus)*	Hs.21016	2.635
213568_at	*OSR2*	*Odd-skipped-related 2 (Drosophila)*	Hs.253247	2.535
209719_x_at	*SERPINB3*	*Serpin peptidase inhibitor, clade B (ovalbumin), member 3*	Hs.227948	2.498
209720_s_at	*SERPINB3*	*Serpin peptidase inhibitor, clade B (ovalbumin), member 3*	Hs.227948	2.412
1554242_a_at	*COCH*	*Coagulation factor C homolog, cochlin (Limulus polyphemus)*	Hs.21016	2.332
205713_s_at	*COMP*	*Cartilage oligomeric matrix protein*	Hs.1584	2.277
206643_at	*HAL*	*Histidine ammonia-lyase*	Hs.190783	2.233
206177_s_at	*ARG1*	*Arginase, liver*	Hs.440934	2.229
206426_at	*MLANA*	*Melan-A*	Hs.154069	2.085
206630_at	*TYR*	*Tyrosinase (oculocutaneous albinism IA)*	Hs.503555	2.027
213880_at	*LGR5*	*Leucine-rich repeat-containing G protein-coupled receptor 5*	Hs.658889	2.009
206140_at	*LHX2*	*LIM homeobox 2*	Hs.696425	1.997
206427_s_at	*MLANA*	*Melan-A*	Hs.154069	1.966
210095_s_at	*IGFBP3*	*Insulin-like growth factor-binding protein 3*	Hs.450230	1.953
(B) Downregulated				
239272_at	*MMP28*	*Matrix metallopeptidase 28*	Hs.380710	0.714
236035_at	—	*Transcribed locus*	Hs.435027	0.714
223437_at	*PPARA*	*Peroxisome proliferator-activated receptor alpha*	Hs.103110	0.714
203972_s_at	*PEX3*	*Peroxisomal biogenesis factor 3*	Hs.7277	0.713
218552_at	*ECHDC2*	*Enoyl Coenzyme A hydratase domain containing 2*	Hs.476319	0.712
209048_s_at	*ZMYND8*	*Zinc finger, MYND-type containing 8*	Hs.446240	0.712
226560_at	—	*Transcribed locus*	Hs.210043	0.711
238567_at	*SGPP2*	*Sphingosine-1-phosphate phosphatase 2*	Hs.591604	0.709
221942_s_at	*GUCY1A3*	*Guanylate cyclase 1, soluble, alpha 3*	Hs.24258	0.708
213935_at	*ABHD5*	*Abhydrolase domain containing 5*	Hs.655670	0.708
210512_s_at	*VEGFA*	*Vascular endothelial growth factor A*	Hs.73793	0.707
228221_at	*SLC44A3*	*Solute carrier family 44, member 3*	Hs.483423	0.706
225726_s_at	*PLEKHH1*	*Pleckstrin homology domain containing, family H (with MyTH4 domain) member 1*	Hs.594236	0.703
225728_at	*SORBS2*	*Sorbin and SH3 domain containing 2*	Hs.655143	0.703
206605_at	*P11*	*26 Serine protease*	Hs.997	0.703
217523_at	*CD44*	*CD44 molecule (Indian blood group)*	Hs.502328	0.703
225755_at	*KLHDC8B*	*Kelch domain containing 8B*	Hs.13781	0.703
229147_at	—	*Transcribed locus*	Hs.529677	0.703
212463_at	*CD59*	*CD59 molecule, complement regulatory protein*	Hs.278573	0.702
240038_at	—	*Transcribed locus*	Hs.608694	0.702

Table 2. The functional classes of differentially expressed genes

Putative function	*P*-value	Gene symbol	Gene title	Fold induction (geom. mean)
Melanin biosynthetic process	1.2×10^{-6}	*DCT*	*Dopachrome tautomerase (tyrosine-related protein 2)*	1.646
		SILV	*Silver homolog (mouse)*	3.040
		TYR	*Tyrosinase*	2.027
		TYRP1	*Tyrosinase-related protein 1*	2.881
Lipid metabolic process	2.5×10^{-5}	*DHRS9*	*Dehydrogenase/reductase (SDR family) member 9*	0.598
		EBP	*Emopamil-binding protein (sterol isomerase)*	0.683
		PPARGC1A	*Peroxisome proliferator-activated receptor gamma, coactivator 1 alpha*	0.688
		SLC27A2	*Solute carrier family 27 (fatty acid transporter), member 2*	0.590
		DGAT2L3	*Diacylglycerol O-acyltransferase 2-like 3*	0.575
		ALOX15B	*Arachidonate 15-lipoxygenase, type B*	0.480
		HACL1	*2-Hydroxyacyl-CoA lyase 1*	0.672
		HMGCS1	*3-Hydroxy-3-methylglutaryl-Coenzyme A synthase 1 (soluble)*	0.667
		HMGCS2	*3-Hydroxy-3-methylglutaryl-Coenzyme A synthase 2 (mitochondrial)*	0.676
		HPGD	*Hydroxyprostaglandin dehydrogenase 15-(NAD)*	1.449
		HSD11B1	*Hydroxysteroid (11-beta) dehydrogenase 1*	0.616
		ACADM	*Acyl-Coenzyme A dehydrogenase, C-4 to C-12 straight chain*	0.678
		MVD	*Mevalonate (diphospho) decarboxylase*	0.680
		RDH11	*Retinol dehydrogenase 11 (all-*trans*/9-*cis*/11-*cis*)*	0.668
		PPARA	*Peroxisome proliferator-activated receptor alpha*	0.714
		PPARA	*Peroxisome proliferator-activated receptor alpha*	0.695
		PECR	*Peroxisomal* trans*-2-enoyl-CoA reductase*	0.625
		ACSS2	*Acyl-CoA synthetase short-chain family member 2*	0.643
		PTGIS	*Prostaglandin I2 (prostacyclin) synthase*	1.387
		PTGS1	*Prostaglandin-endoperoxide synthase 1*	1.480
		PTGS1	*Prostaglandin-endoperoxide synthase 1*	1.542
		SULT1E1	*Sulfotransferase family 1E, estrogen-preferring, member 1*	1.833
Prostaglandin metabolic process	1.9×10^{-3}	*PTGIS*	*Prostaglandin I2 (prostacyclin) synthase*	1.387
		PTGS1	*Prostaglandin-endoperoxide synthase 1*	1.480
		PTGS1	*Prostaglandin-endoperoxide synthase 1*	1.542

rather than to an increase in the number of pigment-producing cells.

In the present study, 279 genes were found to be modulated in lesional skin. The degrees of these expressional changes were relatively small, which is not surprising considering the immunohistochemical and clinical characteristics of melasma. Importantly, we identified four upregulated melanogenesis-associated genes, including our positive control *TYRP1*, in lesional skin. Of particular interest, we found that a subset of Wnt pathway modulators (Wnt5a, SFRP2, and WIF1) were upregulated in lesional skin. The Wnt pathway has a critical role in the development of epidermal melanocytes, and MITF is a nuclear mediator of this pathway (Takeda *et al.*, 2000; Chien *et al.*, 2009). However, the roles of Wnt proteins and of secreted Wnt inhibitors on cutaneous pigmentation are largely unknown, although a microarray analysis of solar lentigo identified the upregulation of the *SFRP1* gene (Goyarts *et al.*, 2007). Furthermore, a transcriptomic study using palmoplantar skin fibroblasts demonstrated the differential expression of DKK1, an inhibitor of Wnt signaling pathway (Yamaguchi *et al.*, 2009). The findings of these studies suggest that modulation of the Wnt signaling pathway might be involved in the pathogenesis of pigmentary disorders. Our transcriptomic study showed that *WIF1*, *SFRP2,* and *Wnt5a* were upregulated in melasma lesions, and *WIF1* was one of the 20 most upregulated genes. Interestingly, our immunohistochemical analysis demonstrated that WIF1 and Wnt5a proteins were expressed in melanocytes, suggesting that they have a role in melanocyte biology and melanogenesis. The increased SFRP2

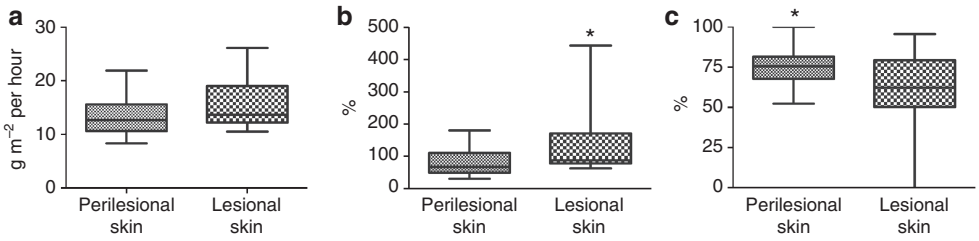

Figure 3. Comparison of the barrier functions of lesional and perilesional skins. (**a**) Basal transepidermal water loss (TEWL) was not significantly different in lesional and perilesional skins. (**b**) TEWL values after barrier perturbation were significantly higher for lesional skin. (**c**) A significantly delayed barrier recovery rate was demonstrated by lesional skin. *$P<0.05$.

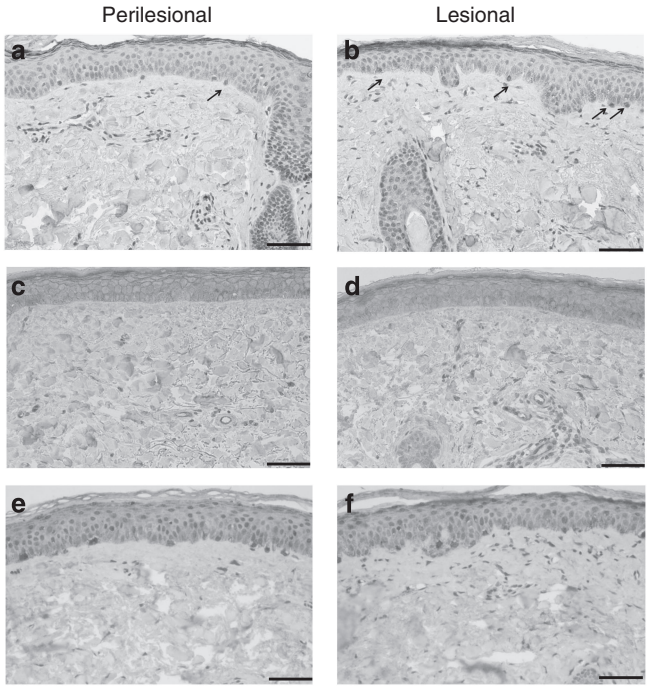

Figure 4. Immunohistochemical staining of Wnt signaling-associated factors. WNT inhibitory factor 1 (WIF1), secreted frizzled-related protein 2 (SFRP2), and Wnt5a were immunohistochemically detected using specific antibodies. Protein levels of WIF1 were greater in melanocytes of lesional skin (**a**) than in those of perilesional skin (**b**). SFRP2 immunoreactivity around fibroblasts in the dermis seemed to be greater in lesional skin than in perilesional skin (**c**, **d**). Wnt5a showed greater expression in the basal layer and around fibroblasts in lesional skin (**e**) than in perilesional skin (**f**) (bar = 200 μm).

immunoreactivity observed around fibroblasts in lesional dermis also suggested the possibility of cross talk between the dermis and epidermis via the Wnt pathway during the development of melasma. Further studies are necessary to elucidate the role of Wnt signaling modulators in cutaneous pigmentation.

Our bioinformatics analysis identified significant modifications of lipid metabolism-related genes in melasma. Also, we found that the barrier function of lesional skin is easily damaged and that it has a delayed recovery rate as compared with perilesional skin. The mechanisms underlying this abnormal barrier function in melasma are not clear, but it is well known that lipids of the stratum corneum have an important role in barrier homeostasis, and thus, the down-regulation of lipid genes in melasma may be related to an impaired barrier function. Furthermore, previous studies have demonstrated that chronic UV exposure, which is an aggravating factor in melasma, influences cutaneous fatty acid metabolism and skin barrier function (Merle *et al.*, 2010). Therefore, an altered barrier function in melasma might be a result of the chronic UV exposure and accompanying epidermal hyperpigmentation. Interestingly, recent studies have demonstrated that barrier function is also influenced by pigmentation (Gunathilake *et al.*, 2009). The biological role of lipid metabolism in the pathogenesis of melasma remains an interesting topic for future study. Furthermore, improvement in epidermal barrier function may be an unrecognized factor to be considered in treating melasma.

Prostaglandin biosynthesis is also significantly modified in the lesional skin of melasma. Prostaglandins are synthesized in the skin in response to UV exposure, and are known to affect melanogenesis (Rhodes *et al.*, 2009). It has also been clinically documented that prostaglandin analogs induce epidermal hyperpigmentation (Kapoor *et al.*, 2009). Interestingly, gene expression profiling analysis of solar lentigo demonstrated the upregulations of genes related to fatty acid metabolism, which suggested the activation of the arachidonic acid pathway (Aoki *et al.*, 2007).

UV exposure is believed to be an aggravating factor in melasma, and previous studies have indicated that melasma lesions show a higher degree of UV-induced damage, similar to solar elastosis (Hernández-Barrera *et al.*, 2008). In the present study, we noted that the expressions of some genes previously demonstrated to be associated with UV exposure were altered in lesional skin. These genes include *MITF* and the melanogenesis-associated genes *TYR*, *TYRP1*, and *DCT*, which were all found to be upregulated in UV-irradiated human skin *in vivo* (Suzuki *et al.*, 2002). *SCCA1*, which was found to be increased in human epidermis following UVB exposure (Enk *et al.*, 2004), was also found to be increased in the present study. Furthermore, the redistribution of melanosomes along dendrites and their subsequent transfer to keratinocytes is a known UVR response (Boissy, 2003). The expression of *myosin 5a*), a genes involved in melanosome movement, was increased in lesional skin. Interestingly, the well-known keratinocyte-derived growth factors of

melanocytes, such as *pro-opiomelanocortine* (precursor of MSHs and ACTH), *endothelin 1*, and *basic fibroblast growth factor*, which are induced by acute UV exposure, did not exhibit any significant mRNA changes in lesional skin. Furthermore, the expression of the hallmark UV-responsive gene, *p53,* was unchanged in melasma lesions, which is consistent with the finding that UVR-induced p53 protein increases are principally due to post-translational stabilization rather than transcriptional regulation (Yang *et al.*, 2006).

Recent studies have suggested the involvements of dermal factors in the pathogenesis of melasma (Kang *et al.*, 2006; Kim *et al.*, 2007). In the present study, we observed the upregulation of several angiogenesis-related genes, such as *angiopoietin-like 1* and *2*, *heparanase*, and *MMP2* in lesional skin. However, one of the major angiogenesis-inducing factor, *vascular endothelial growth factor,* was downregulated. Furthermore, *COMP* and *IGFBP3*, which have been detected by gene expression profiling studies of fibroproliferative disorders (Hesselstrand *et al.*, 2008; Smith *et al.*, 2008), were present on our top 20 upregulated genes list. However, the biological roles played by these genes in cutaneous pigmentation are unknown.

It is also believed that sex hormones such as estrogen are involved in the pathogenesis of melasma, and therefore, we expected to observe the upregulations of sex hormones or sex hormone metabolism-related genes. However, in the event only one gene, *estrogen sulfotransferase 1E, member 1,* a major contributor to beta estradiol inactivation, was present on our upregulated genes list.

It was noted that in the present study, gene expression levels were variable in the skin samples, even for the melanogenesis-associated genes. It have been previously reported that some melasma patients have hyperactive melanocytes, which suggests that the statuses of melanocytes differ in melasma patients (Kang *et al.*, 2010). This finding requires further investigation as it might help to explain why patients respond differently to the standard melasma treatment.

In conclusion, our results show that in melasma lesions, melanogenesis in melanocytes is activated at least partially at the transcriptional level. Furthermore, we identified several signaling pathways, including the Wnt signaling and lipid metabolism pathways, potentially involved in the development of melasma lesions. Furthermore, our study provides a first transcriptomic data set for melasma, which should be useful for those attempting to elucidate the pathogenesis of this disease.

MATERIALS AND METHODS

Patients and study design

This study was approved by the South Mediterranean human subject protection committee (Comité de Protection des Personnes Sud Méditerranée II) and by the Institutional Review Board at Ajou University Hospital and was conducted in accordance with the latest revision of the Declaration of Helsinki Principles. For the histological study, skin biopsies were obtained from 10 Caucasian melasma patients of mean age 39.5 years (range 33–47 years). Three patients were eliminated from analyses because of an inadequate melanin in lesional skin. For the transcriptomic study, 12 Korean melasma patients of mean age 43 years (range 30–50 years) were enrolled. An additional set of eight Korean melasma patients were recruited for the immunohistochemical staining of factors identified during the transcriptomic analysis. Another 16 Korean melasma patients were recruited (mean age 44 years; range 31–55 years) to measure skin barrier functions. Informed consent was obtained from all subjects. Exclusion criteria included use of medication for the treatment of melasma and facial diseases including acne and wrinkles during the previous 3 months, the use of steroid containing agents, bleaching products, or retinoic acid-containing agents, any UV or physical therapy (including lasers, dermabrasion, and chemical peeling) during the previous 3 months, or a positive reaction for hepatitis B, C, and HIV. Colors of lesional or perilesional skin were measured using a colorimeter (Chromameter CR300, Minolta, Tokyo, Japan). Two-millimeter punch biopsies from lesional and perilesional normal facial skin (usually within 1 cm away from the lesional border, referred to as perilesional skin) were obtained from each patient under local anesthesia.

Histochemistry/immunohistochemistry and *in situ* hybridization

Hematoxylin–Eosin staining and Fontana–Masson staining were performed using standard protocols. The following antibodies were used for the immunohistochemical evaluation of proteins; TYR (Novocastra, Newcastle upon Tyne, UK), TYRP1 (Novocastra, Wetzlar, Germany), DCT (Santa Cruz Biotechnology, Santa Cruz, CA), SILV, MITF (both from Novocastra, Wetzlar, Germany), SOX10 (Santa Cruz Biotechnology), WIF1 (1:10 dilution; R&D Systems, Minneapolis, MN), SFRP2 (1:30; Sigma Chemical, St Louis, MO), and Wnt5a (Abcam, Cambridge, MA). IHC was performed using a Discovery XT (Ventana, Tucson, AZ) following the manufacturer's protocol for TYR, TYRP1, DCT, SILV, MITF, and SOX10; WIF1, SFRP2, and Wnt5a were detected using a biotinylated secondary antibody and AEC chromogen (Immunogen, Pittsburgh, PA). A DIG-labeled RNA probe against TYRP1 was created by *in vitro* transcription following a standard protocol. ISH was performed using the Discovery XT (Ventana) using a standard protocol. The images were analyzed using MatLab (MathWorks, Natick, MA).

RNA extraction

A total of 12 matched tissue pairs were immediately frozen in liquid nitrogen. Tissue lysates were homogenized using QIAshredder columns (Qiagen, Valencia, CA) and total RNA samples were obtained using RNeasy micro-kits (Qiagen, Hilden, Germany). DNase I treatment (27 U, 15 minutes) of total RNA was performed directly on the spin columns to eliminate genomic DNA contamination. RNA quantification was performed using the Quant-it Ribogreen RNA assay kit (Molecular Probes, Eugene, OR) and the quality was monitored by following electrophoresis behavior using an Agilent Bioanalyzer 2100 system (Agilent Technologies, Palo Alto, CA). Extracted RNA (50 ng) of good quality (RNA integrity number $\geqslant 7$) was then used for probe synthesis.

Affymetrix probe synthesis and hybridization

Total RNA (50 ng) from each sample was used to generate double-stranded complementary DNA (cDNA) using a T7-oligo (dt) primer

(Two cycle cDNA synthesis kit, Affymetrix, Santa Clara, CA). This cDNA was then used to produce complementary RNA (cRNA) using an *in vitro* transcription kit MEGAscript T7 (Ambion, Austin, TX). cRNA (600 ng) was used for the second round of double-stranded cDNA synthesis (Two cycle cDNA synthesis kit, Affymetrix). The cDNA so obtained was then used to produce biotinylated cRNA using the *in vitro* transcription Gene Chip IVT labelling kit (Affymetrix). Biotinylated cRNA (20 μg) was fragmented and fragmented cRNA (15 μg) was hybridized to an Affymetrix human U133A 2.0 plus microarray (Affymetrix). Arrays were processed on a Gene Chip Fluidics Station 450 and scanned on an Affymetrix Gene Chip Scanner 3000 (Affymetrix). Raw data were analyzed using a GeneChip Expression Consol (Affymetrix) using the robust multi-array average method. The skin samples of two patients did not pass quality controls, and were excluded from further analysis, which was performed using 10 paired samples.

Statistical analysis

Probe sets with at least two in four insignificant calls were disregarded, which resulted in 27,642 of 54,675 probe sets being considered for the statistical analysis. For each subject, the mean expression ratio of lesional to perilesional samples was subtracted from each of the four expression values measured on each probe set to cancel inter-individual validations. The Student's *t*-test was applied on subject-corrected expression values along with Benjamini–Hochberg adjustment for multiplicity testing. The first statistical analysis of 10 paired samples showed that 131 probe sets were differentially expressed in lesional and perilesional skin. Hierarchical clustering was performed on these 131 probe sets and identified a subgroup of six patients who were more strongly affected in terms of gene expressional changes than the other four patients. A second statistical analysis on the six paired samples identified 339 probe sets. The 339 probe sets were used for bioinformatics analysis.

Bioinformatics analysis

GOTM (http://bioinfo.vanderbilt.edu/gotm/), a gene ontology enrichment analysis tool, was used to obtain biologically meaningful information based on gene lists (Zhang *et al.*, 2004). This tool compares a user-uploaded gene list with all gene ontology categories to identify those with an enriched number of user-uploaded genes. The result is visualized in a directed acyclic graph in order of maintaining relationship among the enriched gene ontology categories.

To investigate possible biological interactions of differentially regulated genes, the gene lists derived by statistical analyses were exported into the Ingenuity Pathway Analysis Tool (IPA Tool; Ingenuity Systems, Redwood City, CA; http://www.ingenuity.com).

Skin barrier function

The basal TEWL was measured on both lesional and non-lesional skin using a Tewameter probe (TM210; connected to MPA-5, Courage + Khazaka Electronic GmbH, Köln, Germany). To determine barrier recovery rates, barrier perturbation was performed five times by repeated tape stripping (D-Squame), and TEWL values were measured immediately (T_{imm}) and 5 hours after barrier perturbation ($T_{5\,hours}$). Barrier recovery rates were calculated using $(T_{imm} - T_{5\,hours})/(T_{imm} - T_{base}) \times 100$. All subjects rested for 30 minutes in the 24–26 °C/50–55% RH testing environment before basal TEWL was measured.

CONFLICT OF INTEREST

The authors state no conflict of interest.

ACKNOWLEDGMENTS

This work was supported by grants of the Korean Health Technology R&D project, Ministry for Health, Welfare and Family Affairs, Republic of Korea (A100179), the GRRC Project of Gyeonggi Provincial Government, Republic of Korea, and the Korean Science and Engineering Foundation (KOSEF) Grant funded by the Korean government (MOST) (R13-2003-019) to HY Kang. We thank Carol Chomat for organizing the clinical study.

SUPPLEMENTARY MATERIAL

Supplementary material is linked to the online version of the paper at http://www.nature.com/jid

REFERENCES

Aoki H, Moro O, Tagami H *et al.* (2007) Gene expression profiling analysis of solar lentigo in relation to immunohistochemical characteristics. *Br J Dermatol* 156:1214–23

Boissy RE (2003) Melanosome transfer to and translocation in the keratinocyte. *Exp Dermatol* 12(Suppl 2):5–12

Chien AJ, Conrad WH, Moon RT (2009) A Wnt survival guide: from flies to human disease. *J Invest Dermatol* 129:1614–27

Edmondson SR, Thumiger SP, Kaur P *et al.* (2005) Insulin-like growth factor binding protein-3 (IGFBP-3) localizes to and modulates proliferative epidermal keratinocytes *in vivo*. *Br J Dermatol* 152:225–30

Enk CD, Shahar I, Amariglio N *et al.* (2004) Gene expression profiling of *in vivo* UVB-irradiated human epidermis. *Photodermatol Photoimmunol Photomed* 20:129–37

Garcia MI, Ghiani M, Lefort A *et al.* (2009) LGR5 deficiency deregulates Wnt signaling and leads to precocious Paneth cell differentiation in the fetal intestine. *Dev Biol* 331:58–67

Goyarts E, Muizzuddin N, Maes D *et al.* (2007) Morphological changes associated with aging: age spots and the microinflammatory model of skin aging. *Ann N Y Acad Sci* 1119:32–9

Grimes PE, Yamada N, Bhawan J (2005) Light microscopic, immunohistochemical, and ultrastructural alterations in patients with melasma. *Am J Dermatopathol* 27:96–101

Gunathilake R, Schurer NY, Shoo BA *et al.* (2009) pH-regulated mechanisms account for pigment-type differences in epidermal barrier function. *J Invest Dermatol* 129:1719–29

Hernández-Barrera R, Torres-Alvarez B, Castanedo-Cazares JP *et al.* (2008) Solar elastosis and presence of mast cells as key features in the pathogenesis of melasma. *Clin Exp Dermatol* 33:305–8

Hesselstrand R, Kassner A, Heinegård D *et al.* (2008) COMP: a candidate molecule in the pathogenesis of systemic sclerosis with a potential as a disease marker. *Ann Rheum Dis* 67:1242–8

Im S, Kim J, On WY *et al.* (2002) Increased expression of alpha-melanocyte-stimulating hormone in the lesional skin of melasma. *Br J Dermatol* 146:165–7

Kang HY, Bahadoran P, Suzuki I *et al.* (2010) *In vivo* reflectance confocal microscopy detects pigmentary changes in melasma at a cellular level resolution. *Exp Dermatol* 19:e228–33

Kang HY, Hwang JS, Lee JY *et al.* (2006) The dermal stem cell factor and c-kit are overexpressed in melasma. *Br J Dermatol* 154:1094–9

Kang WH, Yoon KH, Lee ES *et al.* (2002) Melasma: histopathological characteristics in 56 Korean patients. *Br J Dermatol* 146:228–37

Kapoor R, Phiske MM, Jerajani HR (2009) Evaluation of safety and efficacy of topical prostaglandin E2 in treatment of vitiligo. *Br J Dermatol* 160:861–3

Kawano Y, Kypta R (2003) Secreted antagonists of the Wnt signalling pathway. *J Cell Sci* 1:2627–34

Kim EH, Kim YC, Lee ES *et al.* (2007) The vascular characteristics of melasma. *J Dermatol Sci* 46:111–6

Merle C, Laugel C, Baillet-Guffroy A (2010) Effect of UVA or UVB irradiation on cutaneous lipids in films or in solution. *Photochem Photobiol* 86:553–62

Ortonne JP, Arellano I, Berneburg M *et al.* (2009) A global survey of the role of ultraviolet radiation and hormonal influences in the development of melasma. *J Eur Acad Dermatol Venereol* 23:1254–62

Rhodes LE, Gledhill K, Masoodi M *et al.* (2009) The sunburn response in human skin is characterized by sequential eicosanoid profiles that may mediate its early and late phases. *FASEB J* 23:3947–56

Smith JC, Boone BE, Opalenik SR *et al.* (2008) Gene profiling of keloid fibroblasts shows altered expression in multiple fibrosis-associated pathways. *J Invest Dermatol* 128:1298–310

Suzuki I, Kato T, Motokawa T *et al.* (2002) Increase of pro-opiomelanocortin mRNA prior to tyrosinase, tyrosinase-related protein 1, dopachrome tautomerase, Pmel-17/gp100, and P-protein mRNA in human skin after ultraviolet B irradiation. *J Invest Dermatol* 118:73–8

Takeda K, Yasumoto K, Takada R *et al.* (2000) Induction of melanocyte-specific microphthalmia-associated transcription factor by Wnt-3a. *J Biol Chem* 275:14013–6

Yamaguchi Y, Morita A, Maeda A *et al.* (2009) Regulation of skin pigmentation and thickness by Dickkopf 1 (DKK1). *J Investig Dermatol Symp Proc* 14:73–5

Yang G, Zhang G, Pittelkow MR *et al.* (2006) Expression profiling of UVB response in melanocytes identifies a set of p53-target genes. *J Invest Dermatol* 126:2490–506

Zhang B, Schmoyer D, Kirov S *et al.* (2004) GOTree Machine (GOTM): a web-based platform for interpreting sets of interesting genes using Gene Ontology hierarchies. *BMC Bioinformatics* 5:16